Binding of Cationic Porphyrin to Isolated and Encapsidated Viral DNA Analyzed by Comprehensive Spectroscopic Methods†

Kristóf Zupán,‡ Levente Herényi,‡ Katalin Tóth,§ Zsuzsa Majer,|| and Gabriella Csík*,⊥

Institute of Biophysics and Radiation Biology, Semmelweis University, Budapest, Hungary, Biophysik der Makromoleküle, DKFZ, Heidelberg, Germany, Department of Organic Chemistry, Eötvös Loránd University, Budapest, Hungary, and Research Group for Biophysics, Hungarian Academy of Science, Semmelweis University, Budapest, Hungary

Received March 8, 2004; Revised Manuscript Received May 18, 2004

ABSTRACT: The complexation of tetrakis(4-*N*-methylpyridyl)porphyrin (TMPyP) with free and encapsidated DNA of T7 bacteriophage was investigated. To identify binding modes and relative concentrations of bound TMPyP forms, the porphyrin absorption spectra at various base pair/porphyrin ratios were analyzed. Spectral decomposition, fluorescent lifetime, and circular dichroism measurements proved the presence of two main binding types of TMPyP, e.g., external binding and intercalation both in free and in encapsidated DNA. Optical melting studies revealed that TMPyP increases the strand separation temperature of both free and native phage DNA and does not change the phase transition temperature of phage capsid proteins. From these findings we concluded that TMPyP binding does not influence the protein structure and/or the protein−DNA interaction. A combined analysis of absorption spectra and fluorescence decay curves made possible the determination of concentrations of free, externally bound, and intercalated porphyrin. As a perspective, our results facilitate a qualitative analysis of the TMPyP binding process at various experimental conditions.

One of the reasons for recent interest in porphyrin−nucleic acid interaction is for the purpose of developing a DNA-specific photosensitizer for photodynamic virus inactivation (*1*, *2*). Recently, it has been found that tri- and tetracationic porphyrins can be applied as effective photoactivated agents for pathogen reduction in red blood cell concentrates (*3*). Cationic porphyrins are potential candidates for this application, because photodamage can be induced to DNA by sensitizers binding to it or by sensitizers localized in its vicinity (*4*, *5*).

Since the first report of Fiel and co-workers (*6*), the interaction of synthetic nucleic acids with tetracationic *meso*-tetrakis(4-*N*-methylpyridyl)porphyrin (TMPyP)[1] and several of its metal derivatives has been studied in detail (*7*−*9*). Cationic porphyrins which can attain a planar configuration are considered to bind noncovalently to DNA by two distinct mechanisms: intercalation between base pairs or external binding in a groove. Several studies have shown that TMPyP exhibits sequence selectivity: the binding to AT regions is nonintercalative whereas truly intercalated species require GC base pairs (*10*−*12*). Spectroscopic properties, such as hypochromicity, absorption, and CD maxima, and fluorescence intensity of TMPyP in the presence of either poly[d(G-C)] or poly[d(A-T)] have been described (*13*). Binding constants of TMPyP to homogeneous DNAs have also been determined by various methods (*8*).

However, the interactions of TMPyP with homogeneous DNAs such as poly[d(G-C)] and poly[d(A-T)] are in principle less complex than those with heterogeneous DNAs such as calf thymus (CT) DNA or a viral genome. Although the binding constant of TMPyP with natural polynucleotide CT DNA has been estimated by several authors, the technique used earlier gives only a global apparent binding constant irrespective of the mode of binding to DNA (*14*−*16*). There are even fewer data about cationic porphyrin−DNA interaction in a multimolecular environment. Some results indicate that TMPyP is localized in the nucleus of the cell (*17*−*19*) or it can be associated to the virus particles in a virus suspension (*20*). However, it is not known how the presence of proteins, e.g., viral capsid proteins or histones, influences the porphyrin−DNA interaction. The analysis of interaction between cationic porphyrins and virus particles prior to irradiation by light seems to be fundamental for the understanding of their photochemical reactions.

The first goal of present work was to develop a method based on the decomposition of TMPyP absorption spectra, which facilitates a quantitative determination of TMPyP species formed in their interaction with a natural double-stranded DNA. Secondly, we investigated whether the presence of protein capsid influences or not the binding of TMPyP to viral DNA.

In our experiments we used double-stranded DNA isolated from bacteriophage T7. Bacteriophage T7 was selected as the nucleoprotein complex (NP). Intraphage T7 DNA exists

† Supported by Grants NATO LST/CLG 977846, ETT 083/2003, and OTKA T 037719.

* To whom correspondence should be addressed. Phone/Fax: 36-1-266-6656. E-mail: csik@puskin.sote.hu.

‡ Institute of Biophysics and Radiation Biology, Semmelweis University.

§ Biophysik der Makromoleküle, DKFZ.

|| Eötvös Loránd University.

⊥ Research Group for Biophysics, Semmelweis University.

[1] Abbreviations: CD, circular dichroism; NP, nucleoprotein complex; SDS, sodium dodecyl sulfate; TMPyP, *meso*-tetrakis(4-*N*-methylpyridyl)porphyrin; Tris, tris(hydroxymethyl)aminomethane.

10.1021/bi0495477 CCC: $27.50
Published on Web 06/19/2004

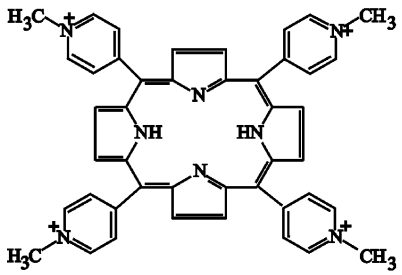

FIGURE 1: Structure of *meso*-tetrakis(4-*N*-methylpyridyl)porphyrin (TMPyP).

in a distorted B-conformation in a quasi-crystalline packing spooled around the core complex (*21*). Isolated DNA undergoes conformational changes concerning the higher order structure and takes a regular B-conformation (*22*). T7 DNA is composed of 40 kilobase pairs and its AT:GC ratio is 1.

EXPERIMENTAL PROCEDURES

meso-Tetrakis(4-N-methylpyridyl)porphyrin (see Figure 1) was purchased from Porphyrin Products (Logan, UT). It was stored at 4 °C in powder form or as a stock solution in distilled water. Before experiments it was diluted to buffer solution composed of 20 mM Tris-HCl and 50 mM NaCl adjusted to pH = 7.4.

T7 Bacteriophage. T7 (ATCC 11303-B7) was grown on *Escherichia coli* (ATCC 11303) host cells. The cultivation and purification were carried out according to the method of Strauss and Sinsheimer (*23*). The phage suspension was concentrated on a CsCl gradient and dialyzed against buffer solution as described above (*24*). The concentration of T7 bacteriophage was determined from its optical density using a molar absorptivity of $\epsilon_{260} = 7.3 \times 10^3$ ($mol_{nucleotide\ bases} \cdot L^{-1} \cdot cm^{-1}$) in phosphate buffer.

Preparation of DNA. DNA was prepared from phages by incubating with 0.5% SDS (Sigma) for 30 min at 65 °C; then the protein−SDS complex was precipitated with 1 M KCl (Sigma) on ice for 10 min (*25*). The precipitate was centrifuged twice for 10 min in an Eppendorf microcentrifuge at 13000 rpm, and then the DNA was precipitated with ethanol from the supernatant. The pellet was washed with 70% ethanol and then suspended in buffer solution, 20 mM Tris-HCl and 50 mM NaCl, pH = 7.4, and the amount of DNA was determined spectrophotometrically. The quality of DNA was checked by electrophoresis and by its absorption spectrum.

Absorption Spectroscopy. Ground-state absorption spectra of TMPyP solutions were recorded with 1 nm steps and 2 nm bandwidth by use of a Cary 4E (Varian, Mulgrave, Australia) spectrophotometer at various DNA or NP concentrations. The composition of solutions was expressed in terms of an *r* number representing the molar ratio of DNA base pairs to TMPyP molecules. Spectral changes due to the adsorption or aggregation of porphyrin were not taken into consideration because the adsorption of TMPyP on the cuvette wall was less than 5% during 30 min and the free porphyrin was in the monomeric state in all samples.

Fitting Procedure. The spectral decomposition was performed for absorption spectra [$A(\lambda)$, absorbance versus wavelength] of the series of TMPyP−DNA and TMPyP−NP solutions with various base pair/porphyrin molar ratios (*r*). All of the spectra were analyzed in the 390−480 nm wavelength range.

For fitting we used the Gaussian multipeaks fit routine from the Microcal Origin software. The error of the fit was determined as

$$\chi^2 = \frac{\sum_{\lambda=390}^{480} [A(\lambda)_{measured} - A(\lambda)_{calculated}]^2}{\sum_{\lambda=390}^{480} A(\lambda)_{measured}} \quad (1)$$

We did not apply the usual wavelength-frequency conversion. The maximum errors of the fitting parameters because of the absence of this conversion were not higher than 0.5 nm.

Fluorescence Experiments. Corrected steady-state emission and excitation spectra were obtained using an FS900CD spectrofluorometer (Edinburgh Analytical Instruments, Edinburgh, U.K.) with a Xe lamp excitation and a Hammamatsu photomultiplier (R955) detection. For the fluorescence lifetime (τ_F) measurements the same instrument was used with a hydrogen-filled flash lamp excitation with 1.5 ns pulse width, and emission decays were determined by the single photon counting method. Samples were excited at the isosbestic wavelength of TMPyP complexes.

Energy Transfer. Contact energy transfer from nucleic acid bases to bound porphyrin was measured from fluorescence excitation and emission spectra recorded between 220 and 330 nm (λ_{em} = 660 nm) and 580−780 nm (λ_{ex} = 260 nm), respectively. The TMPyP concentration was constant in the parallel samples, and the base pair/porphyrin ratio varied between 0 and 30.

Circular Dichroism. Circular dichroism measurements were made on a Jasco J-810 spectropolarimeter calibrated with aminocamphorsulfonic acid at room temperature in 1 cm cells. Spectra were recorded between 380 and 500 nm. Solvent was a buffer consisting of 50 mM Tris and 20 mM NaCl. CD spectra of TMPyP were recorded at various concentrations of the DNA or NP complex. In parallel samples the TMPyP concentration was constant. The spectra were smoothed by the Savitzky−Golay algorithm (*26*).

Optical Melting Measurements. Thermal denaturation curves of the DNA or bacteriophage solutions were recorded by absorbance at 260 nm on a Cary 4E spectrophotometer (Varian, Mulgrave, Australia) equipped with a Peltier thermoregulator. The heating rate was 0.5 °C/min in the temperature range 25−97 °C. Five samples were measured in parallel using an automatic cell changer; the sixth sample holder was used to measure the temperature in an identical quartz cell filled with buffer. The cell holder was insulated to ensure that the temperature did not vary more than 0.1 °C between cells, even above 90 °C. The initial absorbance of the samples were adjusted to approximately 0.2 at 260 nm in quartz cells of 1 cm path length. The absorbance data were collected at every 0.5 °C. Data were treated using the program KaleidaGraph on a Macintosh computer. The curves were normalized to the absorbance at room temperature, smoothed in five-point intervals; derivative melting curves were calculated from the differences between adjacent points as implemented in the program and once more smoothed

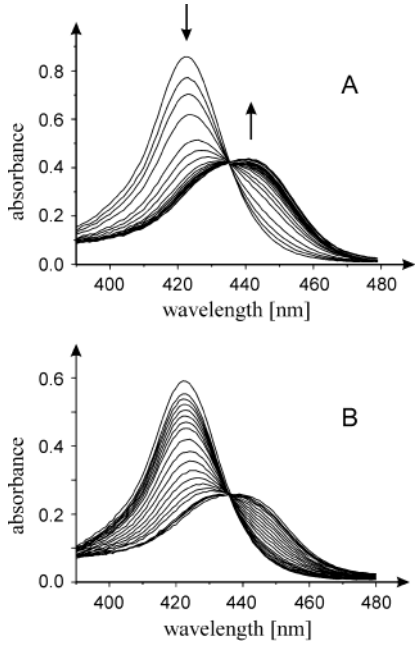

FIGURE 2: Absorption spectra of TMPyP at various concentration of DNA (A) or NP complex (B). Base pair/porphyrin molar ratio (r) varies between 0 and 40.

for five points. The peak of the derivative melting curve was accepted as the corresponding melting temperature (T_m). Another parameter to characterize the transition is its half-width defined on the usual way: the distance between the temperatures, where the derivative reaches half of its extreme value.

RESULTS

Decomposition of Absorption Spectra. Figure 2 shows a series of TMPyP absorption spectra recorded at constant porphyrin and various DNA or NP concentrations. As we can see, increasing relative base pair concentration is followed by hypochromism and red shift of the spectra. These overall spectral changes are typical for the TMPyP−DNA binding described before (*7*, *15*, *27*, *28*).

For further analysis of absorption spectra we made the following assumptions:

(1) All of the measured spectra [$A(\lambda)$] can be considered as a sum of three component spectra belonging to three possible porphyrin states, namely, to free [$A_F(\lambda)$], to externally bound [$A_E(\lambda)$], and to intercalated [$A_I(\lambda)$] porphyrins:

$$A(\lambda) = A_F(\lambda) + A_E(\lambda) + A_I(\lambda) \tag{2}$$

(2) As is interpreted in Figure 3, the spectrum of each state [$A_X(\lambda)$] can be fitted as a sum of two Gaussians, a band [$A_x(\lambda)$] and its shoulder [$A'_x(\lambda)$], that probably correspond to the resonant and nonresonant excitations of the same band:

$$A_X(\lambda) = \frac{A_x}{w_x\sqrt{\pi/2}}\exp\left(\frac{-2(\lambda-\lambda_x)^2}{w_x^2}\right) + \frac{A'_x}{w'_x\sqrt{\pi/2}}\exp\left(\frac{-2(\lambda-\lambda'_x)^2}{w'^2_x}\right) \tag{3}$$

where A_x and A'_x are the total areas under the curves, λ_x, and λ'_x are the centers of the peaks, and w_x and w'_x are the full widths for the band and for the shoulder, respectively.

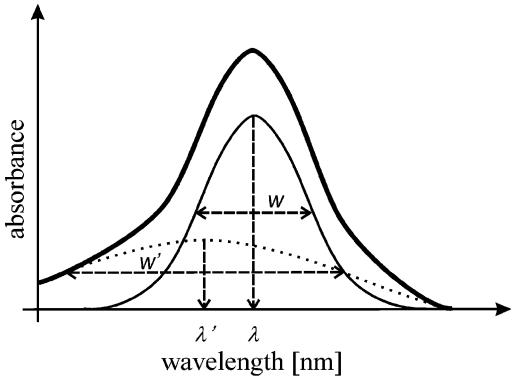

FIGURE 3: Schematic interpretation of spectral decomposition of TMPyP absorption spectrum between 390 and 480 nm: absorption spectrum of one state [$A_X(\lambda)$] (bold line) and its component spectra, main band [$A_x(\lambda)$] (thin line) and its shoulder [$A'_x(\lambda)$] (dotted line). Spectral parameters: the width (w and w') and center of the peak (λ and λ') are indicated.

Table 1: Parameters of the Absorption Spectra of TMPyP Species: Centers (λ_x, λ'_x) and Widths (w_x, w'_x) of Main Absorption Bands and Shoulder; Ratio of Areas under Shoulder and Main Band (α_x), and Molar Absorptivity at the Maximum of the Spectrum (ϵ)

	λ_x (nm)	w_x (nm)	λ'_x (nm)	w'_x (nm)	α_x	ϵ ($M^{-1}\,cm^{-1}$)
free	423	17	415	41	1.32	3.17×10^{-5}
DNA						
external binding	430	20	420	67	1.20	2.98×10^{-5}
intercalation	446	19	420	67	0.80	1.66×10^{-5}
NP						
external binding	430	20	411	73	1.29	2.29×10^{-5}
intercalation	446	19	411	109	1.59	1.34×10^{-5}

(3) The ratio of A'_x to A_x is constant at different populations of one state and can be expressed as

$$\alpha_x = A'_x/A_x \tag{4}$$

(4) The only parameter changing with porphyrin population in a specific state is A_x, and all of the other parameters (α_x, λ_x, λ'_x, w_x, w'_x) are constant for a spectrum belonging to one state.

Spectral parameters of free TMPyP were determined from the spectrum of the DNA-free sample and are given in Table 1. We used these parameters for further fits as constants except the total area (A_f).

From the initial runs of the further fitting procedure, it was recognized that the spectra of the two bound states could be fitted by two main bands and only one common shoulder (A'_c, λ'_c, w'_c). In this way we could reduce the number of parameters, and the remaining unknown parameters were A_f, A_e, A_i, A'_c, λ_e, λ_i, λ'_c, w_e, w_i, and w'_c.

Moreover, by analyzing the results of initial fits we also observed that while the ratios of A_e and A_i were changing with base pair/porphyrin molar ratios, λ'_c and w'_c parameters of the common shoulder practically did not change for the entire series. This is possible only if the centers and the widths of the shoulders of the two bound state spectra are equal to each other ($\lambda'_c = \lambda'_e = \lambda'_i$, $w'_c = w'_e = w'_i$) and

$$A'_c = A'_e + A'_i \tag{5}$$

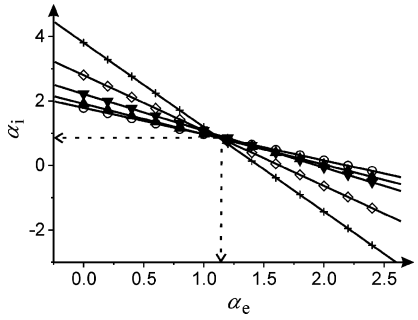

FIGURE 4: α_i as a function of α_e (for interpretation, see eq 4) at various base pair/porphyrin ratios (r): 1.65 (+), 3.63 (◇), 6.05 (▼), 8.81 (▲), and 20.55 (○).

Using eq 4 A'_c can be expressed as a linear combination of A_e and A_i:

$$A'_c = A_e\alpha_e + A_i\alpha_i \quad (6)$$

Thus from eq 6 α_i can be determined as a linear function of α_e:

$$\alpha_i = \frac{A'_c}{A_i} - \frac{A_e}{A_i}\alpha_e \quad (7)$$

From the results of spectral decompositions received for a given base pair/porphyrin ratio the corresponding linear function can be constructed.

We performed the spectral decomposition procedures for several base pair/porphyrin ratios in the range $0 \leq r \leq 40$. From a set of results, received for the same base pair/porphyrin ratio α_i and α_e values were calculated. In Figure 4 we present α_i as a function of α_e and the graphical representation of fitted straight lines received at various r values of TMPyP−DNA solutions. One can recognize that these linear functions have a common point.

One of our initial assumptions is that α_i and α_e are independent of r. This assumption is fulfilled by those α_i and α_e coordinates belonging to the crossing point of the linear functions. These values were accepted as the best α_e and α_i parameters, and they were used as constants in the final fitting procedure. Very similar considerations were made in the analysis of NP-complexed TMPyP absorption spectra. The results of the final fitting runs as for the spectral parameters of TMPyP species are shown in Table 1.

Fluorescence Decay Measurements. As a very sensitive signal of the changes of the environment of the chromophore, the fluorescence lifetime of TMPyP was measured at room temperature. First the fluorescent lifetime of free TMPyP was determined. The isotropic decay of TMPyP in the absence of DNA is monoexponential (data not shown). The lifetime determined from the decay curve is 5.4 ns. This value corresponds to the lifetime of nonbound TMPyP determined by Shen et al. (*29*).

The fluorescence decay of TMPyP was measured and analyzed at various DNA or NP concentrations. The lifetimes of fluorescent TMPyP species obtained at various r numbers are presented in Table 2. Figure 5A shows the fluorescence decay recorded in the presence of isolated DNA at $r = 12$. In this case and whenever r was higher than 8, the best fit was achived by a biexponential function. The lifetime components are around 10.4 and 2.8 ns. These values are in good agreement with the lifetimes of intercalated and externally bound TMPyP determined by Shen et al. (*29*). On the basis of this conformability, we identify the shorter lifetime as belonging to the intercalated species and the longer one as belonging to externally bound TMPyP.

Table 2: Fluorescence Lifetimes (τ) and Relative Concentrations (%) of Porphyrin Species in TMPyP−DNA and TMPyP−NP Solutions at Various Base Pair/Porphyrin Molar Ratios (r)

	r	τ_1 (ns)	%	τ_2 (ns)	%	τ_3 (ns)	%
free	0	5.4 ± 0.3					100
DNA	3.6	5.4 ± 0.2	35	10.4 ± 0.5	32.5	2.6 ± 0.3	32.5
	8			10.3 ± 0.4	34	2.7 ± 0.4	66
	12			10.2 ± 0.5	29	2.8 ± 0.3	69.5
NP	18	5.4 ± 0.5	38	7.3 ± 0.3	33	2.3 ± 0.4	29
	27	5.4 ± 0.3	12	7.4 ± 0.8	44	2.7 ± 0.2	44

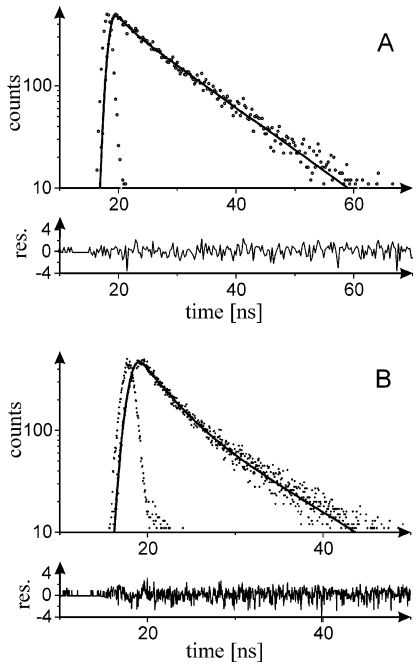

FIGURE 5: Fluorescence decay curves of TMPyP in the presence of isolated DNA (A) and NP (B). Base pair/porphyrin ratios are 12 and 27, respectively.

When NP was added to TNPyP, a triexponential decay curve was identified even at $r = 27$ (see Figure 5B). The lifetime components are 2.7, 5.4, and 7.4 ns. The 5.4 ns component indicates that there are free porphyrin molecules even at such high base pair/porphyrin ratio; 2.7 ns is equal to the value identified as the lifetime of intercalated porphyrin in isolated DNA. The third component significantly deviates from the lifetime of TMPyP externally bound to DNA. However, we suppose and later in this work we try to prove that this belongs to a species externally bound to the intraphage DNA.

From the relative contributions of fluorescent species to the fluorescence intensity of a sample, the relative concentrations of free, externally bound, and intercalated TMPyP were determined. These data are shown in Table 2.

Determination of specific absorbance of TMPyP forms was done by combining of spectral decomposition and fluorescent lifetime measurement performed at a similar base pair/porphyrin molar ratio. The concentration of a given TMPyP form was known as a result of a fluorescent decay experiment. The corresponding absorbance of the same TMPyP

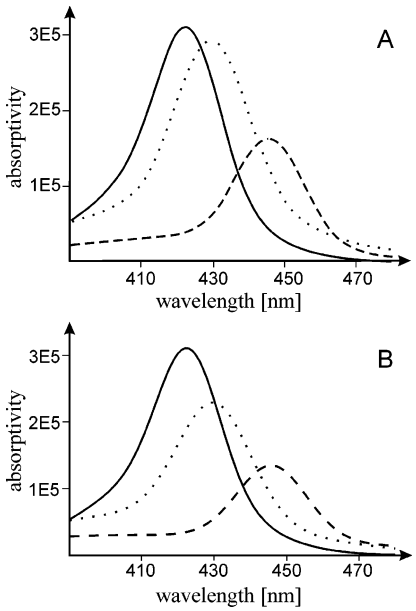

FIGURE 6: Reconstructed specific absorbance spectra of TMPyP species in the presence of isolated DNA (A) and NP (B): free (solid line), externally bound (dotted line), and intercalated (dashed line) TMPyP.

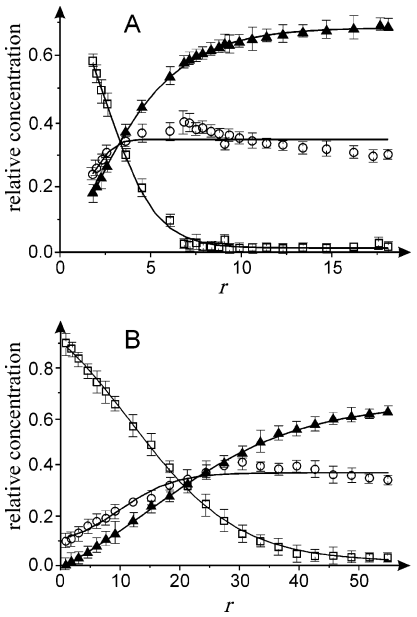

FIGURE 7: Distribution of TMPyP between free (□), externally bound (○), and intercalated (▲) states as a function of base pair/porphyrin molar ratio (*r*) in DNA (A) and NP complex (B). Lines have been fitted by Microcal Origin sigmoid fit.

form was determined by decomposition of the absorption spectrum. Calculated specific absorbances at the absorption maxima of TMPyP species are listed in Table 1. According to these data the hypochromicity due to the external binding is about 6%, and that for intercalation is about 40%.

Knowing the spectral parameters of a TMPyP form and its specific absorbance, the molar absorptivity spectrum can be calculated. These reconstructed molar absorptivity spectra of TMPyP forms are presented in Figure 6. The maxima of the spectra are at 430 and 446 nm for external binding and intercalation, respectively. As we can see, both types of binding lead to a red shift of the absorption spectrum as compared to the free TMPyP. The red shift for the external binding is about 7 nm, and for the intercalation it is 23 nm.

Distribution of TMPyP between Binding States. We recorded the absorption spectra of TMPyP in the presence of isolated DNA or phage NP in a wide range of *r*. After decomposition of absorption spectra, the knowledge of molar absorptivities of TMPyP forms facilitated the determination of contributions of free, externally bound, and intercalated TMPyP at any base pair/porphyrin ratio. These contributions are presented in Figure 7 as the function of *r*. According to our results, the full binding to isolated DNA requires an $r = 7.2 \pm 0.5$. In the case of intraphage DNA *r* must be higher than 30. At higher relative DNA concentrations a slight decrease in externally bound and a parallel increase in intercalated TMPyP concentration can be observed. However, these changes, indicating a redistribution of bound porphyrin, are within the experimental error.

Fluorescence Energy Transfer. Since the first report of contact energy transfer from DNA bases to bound ligands by Le Pecq and Paoletti (*30*), this technique has been used frequently in DNA−ligand interaction studies. Porphyrins that contact closely with DNA bases are characterized by a clear increase of their fluorescence quantum yields for an excitation around 260 nm, corresponding to an energy transfer from DNA bases to porphyrins (*15*). This phenomenon can be considered as a criterion for intercalation.

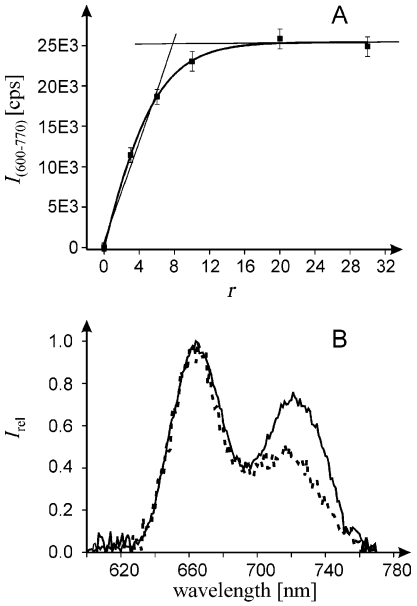

FIGURE 8: (A) Integrated fluorescence intensity of bound TMPyP upon excitation at 260 nm as the function of the DNA base pair/porphyrin molar ratio (*r*). The concentration of TMPyP was 2 μM. (B) Normalized fluorescence spectra of TMPyP corresponding to full binding to isolated DNA (solid line) ($r = 8$) and NP complex (dashed line) ($r = 40$). $\lambda_{ex} = 260$ nm. The porphyrin concentration was 2 μM.

We recorded the fluorescence emission spectra of TMPyP−DNA samples when they were excited at 260 nm. Figure 8A shows the integrated fluorescence intensity of TMPyP (2 μM) at various concentrations of isolated phage DNA. Since the fluorescence intensity of free TMPyP upon excitation at 260 nm is not zero, the emissions of free and bound forms are superimposed. The fluorescence intensity of the bound porphyrin (I_b) can be estimated as

$$I_b = I - I_0 n_f \quad (8)$$

where *I* refers to the measured fluorescence intensity at

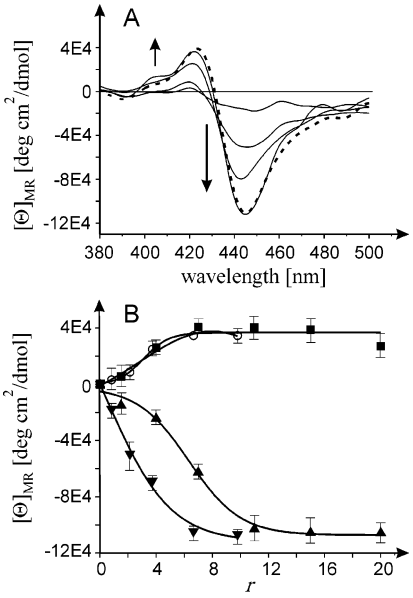

FIGURE 9: (A) CD spectra of TMPyP in the presence of free DNA (solid lines) and NP complex (dashed line); r values are between 0.8 and 6.6 in DNA-containing samples and $r = 15.3$ in NP-containing sample. (B) Molar ellipticity of TMPyP in the presence of DNA (▼, ○) or NP (▲, ■) measured at 422 (○, ■) and 448 (▼, ▲) nm as the function of r.

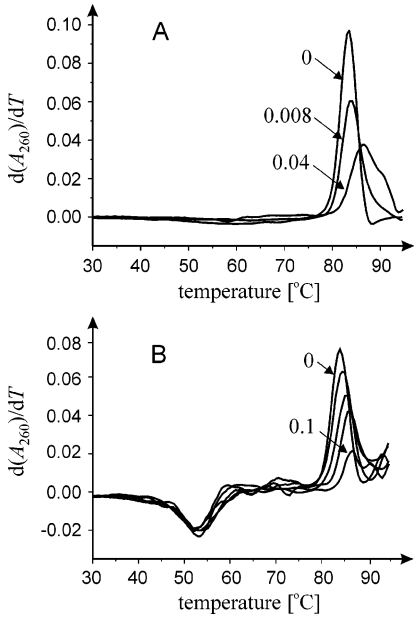

FIGURE 10: Derivative melting curves of isolated T7 DNA (A) and T7 phage (B) at various porphyrin/base pair ratios ($1/r$). The base pair concentration of the samples was about 12 μM; $1/r$ values varied between 0 and 0.04 (A) and 0−0.1 (B), respectively.

various DNA concentrations, I_0 is the fluorescence intensity of DNA-free solution, and n_f is the relative concentration of free TMPyP.

A significant increase in the emitted intensity can be observed at constant porphyrin concentration when the base pair/porphyrin molar ratio is increased up to about 7. Similar changes take place when TMPyP solution is supplemented with the NP complex. However, in this case the saturation of the process can be reached when r is about 30.

Normalized emission spectra ($\lambda_{ex} = 260$ nm) of TMPyP bound to DNA or NP are presented in Figure 8B. This type of presentation has been selected because, besides the emitted intensity, the shape of the emission spectra is also informative. These spectra show good correspondence to each other. In both cases, the emission maxima are at 665 and 722 nm. These values fit to the maxima of the typical emission spectrum of intercalated TMPyP species described by Kelly et al. (*13*). However, the relative amplitudes of two peeks are different in the case of DNA and NP binding.

Circular Dichroism. In addition to absorption and energy transfer measurements, CD study is a useful tool for the diagnostic of the interaction of TMPyP with DNA and the NP complex. Porphyrins, although nonchiral, display induced circular dichroism (CD) spectra in the Soret region when they are bound to DNA (*27*, *28*, *31*, *32*). Figure 9A shows CD spectra of TMPyP recorded in the presence of DNA. The porphyrin concentration was constant and the base pair/porphyrin ratios varied between 0 and 6.6. All spectra are composed of a positive band centered on 422 nm and a negative one around 445 nm. The appearance of a negative induced CD band is a signature for intercalation whereas a positive induced band is indicative of a nonintercalated binding mode (*9*). Ellipticities measured at 422 and 445 nm are presented in Figure 9B as the function of r. They increase up to $r \approx 7$; then the addition of DNA does not result in further change in the amplitudes.

In the CD spectrum induced by the presence of the NP complex, the typical positive and negative spectral bands can be recognized at 422 and 445 nm, respectively. The amplitudes of bands are increasing by increasing NP concentration, and the process is saturated at $r \approx 15$. Figure 9A presents the induced CD spectrum of TMPyP when it is supplemented with the NP complex and r is 15. One can recognize that not only the position of spectral bands but also the highest possible amplitudes are similar in the presence of DNA or NP.

Optical Melting Measurements. The interaction between porphyrin derivatives and DNA or the NP complex can be also recognized due to the stability changes in macromolecules. To look for possible structural changes caused by the TMPyP binding, the thermal stability of the T7 phage and DNA was detected by optical melting; e.g., the thermal denaturation of the whole T7 phage and isolated DNA was monitored via the changes in their absorbance at 260 nm.

The melting derivative curves of DNA and the NP complex recorded at various TMPyP and constant base pair concentrations are presented in panels A and B of Figure 10, respectively. The hyperchromic transition around 84 °C (T_m) is attributed to the denaturation of the DNA double helix: the opening of the H bonds, weakening of the stacking interaction, and the separation of the two single strands. All curves in Figure 10B show two structural transitions typical for the T7 nucleoprotein complex: a hypochromic change between 50 and 60 °C (T_m') and a hyperchromic one around 84 °C. The low-temperature transition is due to the disruption of the phage particle, as has been shown first by electron microscopy (*33*) and confirmed later in solution by the observed decrease in light scattering intensity (*34*). During this transition, the DNA is released from the capsid; it adopts a regular B tertiary structure (*34*) and loses its higher order arrangement (*35*). The high-temperature transition (T_m) is related to the DNA denaturation as described for isolated DNA.

Table 3: Melting Parameters: Melting Temperature and Half-Width of DNA and NP at Various Porphyrin/Base Pair (1/*r*) Ratios[a]

	1/*r*	T_m' (max)	half-width	T_m (max)	half-width
NA	0			82.5 ± 0.8	4.55 ± 0.3
	0.008			84.80 ± 0.7	4.6 ± 0.3
	0.02			85.65 ± 0.8	5.3 ± 0.4
	0.04			87.2 ± 0.6	7.78 ± 0.5
	0.05			88.05 ± 0.5	11.5 ± 0.4
	0.06			89.50 ± 0.8	11.8 ± 0.5
NP	0	53.05 ± 0.5	11.0 ± 0.1	84.0 ± 0.3	4.7 ± 0.5
	0.01	52.5 ± 0.5	11.0 ± 0.2	85.14 ± 0.5	5.1 ± 0.5
	0.03	53.3 ± 0.5	11.5 ± 0.2	85.34 ± 0.4	5.0 ± 0.5
	0.06	53.25 ± 0.5	11.5 ± 0.1	86.0 ± 0.4	5.15 ± 0.5
	0.12	52.5 ± 0.5	10.8 ± 0.4	86.7 ± 0.4	4.3 ± 0.5

[a] The base pair concentration was 20 μM.

Melting Parameters of DNA and the NP Complex. The phase transition temperatures and half-widths measured at various *1/r* values are collected in Table 3. It can be seen that the melting temperature of DNA is shifted to the higher values as the concentration of TMPyP increases, in the case of both free DNA and the NP complex. This means that both types of DNA can interact with TMPyP and the binding of TMPyP results in the stabilization of DNA structure. However, similar TMPyP concentration causes higher temperature shift in free than in intraphage DNA. Besides the stability, the cooperativity of the DNA phase transition is also influenced by the presence of TMPyP, as indicated by the increase of the half-width of derivative curves.

Within experimental error, the melting parameters of phage capsid disruption are constant in the investigated TMPyP concentration range; that is, the presence of TMPyP does not influence the stability of the phage protein capsid. This result suggests that TMPyP does not interact with capsid proteins and does not disturb protein−DNA interaction, even if it has a strong stabilization effect on the intraphage DNA.

DISCUSSION

Our original reason for embarking on an investigation of the interaction of cationic porphyrin with nucleic acids was for the purpose of developing a DNA-specific photosensitizer for photodynamic virus inactivation. Here, the complexation of TMPyP with free and encapsidated DNA of T7 bacteriophage was investigated. T7 phage was selected for two reasons. (1) Samples of both T7 phage and its isolated DNA can be prepared in optical grade purity and in sufficiently high concentration (*36*). That way, two different conformations of the same natural polynucleotide can be investigated. (2) T7 phage can be used as a surrogate of nonenveloped pathogen viruses in the future virus photoinactivation studies performed with cationic porphyrins (*37*).

Under the environmental conditions, temperature, ionic strength, and ionic composition of the buffer solution, used in our experiments, isolated polynucleotide has a regular B-conformation. Intraphage DNA is in close interaction with the protein capsid and the core protein of the phage particle (*21*). Its tertiary structure can be characterized as a distorted B-conformation.

We analyzed the absorption spectra of TMPyP at various base pair/porphyrin ratios in order to identify binding modes and relative concentrations of bound porphyrin forms. When spectra were decomposed to three components, we could find such spectral parameters for component spectra that were independent of the base pair/porphyrin molar ratio. The results of spectral decomposition satisfy the criteria proposed previously (*13*, *27*, *28*): about 20 nm red shift and about 40% hypochromicity of the Soret band for intercalation and a few nanometer red shift and about 5% hypochromicity for external binding. These findings validate our initial assumption that the measured spectra can be considered as a sum of three component spectra belonging to three possible porphyrin states, i.e., free, externally bound, and intercalated porphyrins.

Fluorescence decay experiments also show the presence of two binding states of porphyrin in both TMPyP−DNA and TMPyP−NP complexes. On the basis of lifetime values, one of the bound species can be recognized as intercalated TMPyP in both cases. Energy transfer experiments performed with DNA or NP also prove that TMPyP intercalates between the base pairs of the double helix independently of its secondary or higher ordered structure.

However, the lifetimes of the other binding state differ from each other when DNA or NP is added to the TMPyP solution. In the case of DNA complexation, this value fits to the lifetime of externally bound TMPyP but deviates from it in the case of complexation with NP. This deviation can originate from the different molecular environments of externally bound porphyrins in the two different systems, or it can be an indication for the porphyrin−protein binding in the TMPyP−NP complex.

To clarify the binding modes of TMPyP, the circular dichroism spectra were measured. In general, a single negative band characterizes an intercalated porphyrin (*38*, *39*), and a single positive band belongs to an externally bound porphyrin at DNA grooves (*28*). Our presented observations support the view that TMPyP goes to complex formation with free and encapsidated T7 DNA. From the similarities of CD spectral parameters we can conclude that intercalated and externally bound porphyrin forms are present in both TMPyP−DNA and TMPyP−NP complexes.

Structural changes induced by the porphyrin binding in DNA or NP were also investigated by the optical melting method. Intercalation of molecules into the double helix is known to increase the DNA melting temperature (*38*, *40*). On one hand, it has been found that the presence of TMPyP influences the thermal stability of DNA in both its isolated and encapsidated form, but in the case of NP, higher concentration of TMPyP is needed to reach a similar increase in the strand separation melting temperature. On the other hand, the stability of the phage capsid is not altered even at high base pair/porphyrin ratios, where CD and fluorescence studies already indicate a high relative concentration of both TMPyP binding forms or even full binding of TMPyP. This finding indicates that TMPyP binding to DNA does not involve the protein binding sites of the polynucleotide. According to our previous results, the melting temperature of capsid disruption is shifted to the lower values when the protein−DNA interaction is disturbed either by binding of a molecule or by photochemical damages (*41*, *42*).

On the basis of these results we suggest that the two binding modes of TMPyP in the NP do not include a porphyrin−protein binding but that TMPyP binds to the DNA part of the NP by two distinct binding modes.

The experiments reported here corroborate the evidence that TMPyP interacts with natural polynucleotide. Our results suggest that TMPyP binds to DNA even if the polynucleotide is a part of a nucleoprotein complex. Similar binding forms, i.e., intercalation and outside, nonintercalative binding, can be suggested in both isolated and encapsidated DNA. The presence of the protein capsid in the phage particle does not exclude the interaction between cationic porphyrin and intraphage DNA; however, the full binding of TMPyP can be reached at significantly higher base pair/porphyrin molar ratio. Some spectral properties also indicate that the external binding is influenced by the higher ordered structure of DNA, and the analysis of such differences requires further studies.

The binding model which emerges from these studies confirms earlier views of porphyrin−DNA interaction. We did not see any indication of excitonic species typical when cationic porphyrin is bound either to AT or to GC homopolymers at high binding ratio (*28*).

A combined analysis of absorption spectra and fluorescence decay curves of TMPyP samples enabled us to determine of concentrations of free, externally bound, and intercalated porphyrin. As a perspective, our results facilitate a qualitative analysis of the TMPyP binding process at various experimental conditions such as DNA base composition, DNA conformation, and solvent composition.

Under our experimental conditions, the externally bound species have a higher relative concentration at low base pair/porphyrin molar ratios. The intercalated form becomes dominant when this ratio exceeds 3 or 20 in DNA or NP, respectively. These results correspond to earlier findings (*7*) according to which TMPyP binds to DNA preferentially by intercalation at high DNA/porphyrin ratios. The fraction of porphyrin bound by intercalation decreases as DNA concentration decreases or ionic strength increases with a concurrent shift to outside binding at AT sites.

ACKNOWLEDGMENT

We are very grateful to Professor G. Rontó and Professor J. Langowski for careful reading of the manuscript and to Erzsebet Szakacs for technical assistance.

REFERENCES

1. Kasturi, C., and Platz, M. S. (1992) Inactivation of lambda phage with 658 nm light using a DNA binding porphyrin sensitizer, *Photochem. Photobiol. 56*, 427−429.
2. Wainwright, M. (2003) Local treatment of viral disease using photodynamic therapy, *Int. J. Antimicrob. Agents 21*, 510−520.
3. Trannoy, L. L., Lagerberg, J. W. M., Dubbelman, T. M. A. R., Schuitmaker, H. J., and Brand, A. (2004) Positively charged Porphyrins: a new series of photosensitizers for sterilization of red blood cell concentrates, *Transfusion* (in press).
4. Kvam, E., Stokke, T., and Moan, J. (1990) The lengths of DNA fragments light-induced in the presence of a photosensitizer localized at the nuclear membrane of human cells, *Biochim. Biophys. Acta 1049*, 33−37.
5. Moan, J., and Berg, K. (1991) The photodegradation of porphyrins in cells can be used to estimate the lifetime of singlet oxygen, *Photochem. Photobiol. 53*, 549−553.
6. Fiel, R. J., Howard, J. C., and Datta Gupta, N. (1979) Interaction of DNA with a porphyrin ligand: evidence for intercalation, *Nucleic Acids Res. 6*, 3093−3118.
7. Pasternack, R. F., Garrity, P., Ehrlich, B., Davis, Ch. B., Gibbs, E. J., Orloff, G., Giartosio, A., and Turano, C. (1986) The influence of ionic strength on the binding of water soluble porphyrin to nucleic acid, *Nucleic Acids Res. 14*, 5919−5931.
8. Strickland, J. A., Marzilli, L. G., Gay, K. M., and Wilson, W. D. (1988) Porphyrin and metalloporphyrin binding to DNA polymers: rate and equilibrium binding studies, *Biochemistry 27*, 8870−8878.
9. Sehlstedt, U., Kim, S. K., Carter, P., Goodisman, J., Vollano, J. F., Norden, B., and Dabrowiak, J. C. (1994) Interaction of cationic porphyrins with DNA, *Biochemistry 33*, 417−426.
10. Pasternack, R. F., Gibbs, E. J., and Villafranca, J. J. (1983) Interactions of porphyrins with nucleic acids, *Biochemistry 22*, 2406−2414.
11. Ford, K., Fox, K. R., Neidle, S., and Waring, M. J. (1987) DNA sequence preferences for an intercalating porphyrin compound revealed by footprinting, *Nucleic Acids Res. 15*, 2221−2234.
12. Ford, K. G., Pearl, L. H., and Neidle, S. (1987) Molecular modelling of the interactions of tetra(4-*N*-methylpyridyl)porphyrin with TA and CG sites on DNA, *Nucleic Acids Res. 15*, 6553−6562.
13. Kelly, J. M., Murphy, M. J., McConnell, D. J., and Uigin, C. (1985) A comparative study of the interaction of 5,10,15,20-tetrakis(*N*-methylpyridinium-4-yl)porphyrin and its zinc complex with DNA using fluorescence spectroscopy and topoisomerisation, *Nucleic Acids Res. 13*, 167−184.
14. Sari, M. A., Battioni, J. P., Mansuy, D., and Le-Pecq, J. B. (1986) Mode of interaction and apparent binding constants of meso-tetraaryl porphyrins bearing between one and four positive charges with DNA, *Biochem. Biophys. Res. Commun. 141*, 643−649.
15. Sari, M. A., Battioni, J. P., Dupre, D., Mansuy, D., and Le-Pecq, J. B. (1990) Interaction of cationic porphyrins with DNA: importance of the number and position of the charges and minimum structural requirements for intercalation, *Biochemistry 29*, 4205−4215.
16. Tjahjono, D. H., Akutsu, T., Yoshioka, N., and Inoue, H. (1999) Cationic porphyrins bearing diazonium rings, synthesis and their interaction with calf thymus DNA, *Biochim. Biophys. Acta 1472*, 333−343.
17. Villanueva, A., Juarranz, A., Diaz, V., Gomez, J., and Canete, M. (1992) Photodynamic effects of a cationic mesosubstituted porphyrin in cell cultures, *Anticancer Drug Des. 7*, 297−303.
18. Juarranz, A., Villanueva, A., Canete, M., and Stockert, J. C. (1996) Fluorescent porphyrin counterstaining of chromatin DNA in conjunction with immunofluorescence methods using FITC-labelled antibodies, *J. Microsc. 182*, 46−49.
19. Tobin, W. R., and Greene, R. S. (1999) Meso-substituted cationic porphyrins interact with dsDNA and exhibit different localization patterns in radiation-induced fibrosarcoma cells, *Anticancer Res. 19*, 2953−2958.
20. Jockusch, S., Lee, D., Turro, N. J., and Leonard, E. F. (1996) Photo-induced inactivation of viruses: Adsorption of methylene blue, thionine, and thiopyronine on Qbeta bacteriophage, *Proc. Natl. Acad. Sci. U.S.A. 93*, 7446−7451.
21. Cerritelli, M. E., Cheng, N., Rosenberg, A. H., McPherson, C. E., Booy, F. P., and Steven, A. C. (1997) Encapsidated Conformation of Bacteriophage T7 DNA, *Cell 91*, 271−280.
22. Ronto, Gy., Toth, K., Csik, G., Feigin, L. A., Svergun, D. T., Dembo, A. T., and Shtikova, E. V. (1988) Loosening of the phage structure in a low ionic strength environment, *Eur. Biophys. J. 15*, 293−298.
23. Strauss, J. H., and Sinsheimer, R. L. (1963) Purification and properties of bacteriophage MS2 and of its ribonucleic acids, *J. Mol. Biol. 7*, 43−48.
24. Toth, K., Csik, G., and Ronto, Gy. (1987) Salt effects on the bacteriophage T7- II. Structure and activity changes, *Physiol. Chem. Phys. Med. NMR 19*, 67−74.
25. Fekete, A., Vink, A. A., Gaspar, S., Berces, A., Modos, K., Ronto, G., and Roza, L. (1998) Assessment of the effects of various UV sources on inactivation and photoproduct induction in phage T7 dosimeter, *Photochem. Photobiol. 68*, 527−531.
26. Savitzky, A., and Golay, M. J. E. (1964) Smoothing and differentiation of data by simplified least squares procedures, *Anal. Chem. 36*, 1627−1639.
27. Pasternack, R. F., Bustamante, C., Collings, P. J., Giannetto, A., and Gibbs, E. J. (1993) Porphyrin assemblies on DNA as studied by a resonance light-scattering technique, *J. Am. Chem. Soc. 115*, 5393−5399.
28. Lee, S., Jeon, S. H., Kim, B.-J., Han, S. W., Jang, H. G., and Kim, S. K. (2001) Classification of CD and absorption spectra in the Soret band of H2TMPyP bound to various synthetic polynucleotides, *Biophys. Chem. 92*, 35−45.

29. Shen, Y., Myslinski, P., Treszczanovicz, T., Liu, Y., and Koningstein, J. A. (1992) Picosecond laser-induced fluorescence polarization studies of mitoxantrone and tetrakisporphine/DNA complexes, *J. Phys. Chem. 96*, 7782−7787.
30. Le Pecq, J. B., and Paoletti, J. (1967) A fluorescent complex between ethidium bromide and nucleic acids, *J. Mol. Biol. 27*, 87−106.
31. Lang, K., Anzenbacher, P., Jr., Kapusta, P., Kral, V., Kubat, P., and Wagnerova, D. M. (2000) Long-range assemblies on poly-(dG-dC)$_2$ and poly(dA-dT)$_2$: Phosphonium cationic porphyrins and the importance of the charge, *J. Photochem. Photobiol. B 57*, 51−59.
32. Chen, X., and Liu, M. (2003) Induced chirality of binary aggregates of opposite charged water-soluble porphyrins on DNA matrix, *J. Inorg. Chem. 94*, 106−113.
33. Serwer, P. (1978) A technique for observing extended DNA in negatively stained specimens: observation of bacteriophage T7 capsid-DNA complexes, *J. Ultrastr. Res*. *65*, 112−118.
34. Toth, K., Bolard, J., Ronto, G., and Aslanian, D. (1984) UV-induced small structural changes in the T7 bacteriophage studied by melting methods, *Biophys. Struct. Mech*. *10*, 229−239.
35. Fekete, A., Ronto, G., Feigin, L. A., Tikhonychev, V. V., and Modos, K. (1982) Temperature-dependent structural changes of intraphage T7 DNA, *Biophys. Struct. Mech*. *9*, 1−9.
36. Hegedus, M., Modos, K., Ronto, G., and Fekete, A. (2003) Validation of phage T7 biological dosimeter by quantitative polymerase chain reaction using short and long segments of phage T7 DNA, *Photochem. Photobiol. 78*, 213−219.
37. Egyeki, M., Turóczy, G., Majer, Zs., Tóth, K., Fekete, A., Maillard, Ph., and Csík, G. (2003) Photosensitised inactivation of T7 phage as surrogate of non-enveloped DNA viruses. Efficiency and mechanism of action, *Biochim. Biophys. Acta 1624*, 115−124.
38. Mohammadi, S., Perree-Fauvet, M., Gresh, N., Hillairet, K., and Taillandier, E. (1998) Joint molecular modeling and spectroscopic studies of DNA complexes of a bis(arginyl) conjugate of a tricationic porphyrin designed to target the major groove, *Biochemistry 37*, 6165−6178.
39. Guliaev, A. B., and Leontis, N. B. (1999) Cationic 5,10,15,20-tetrakis(*N*-methylpyridinium-4-yl)porphyrin fully intercalates at 5′-CG-3′ steps of duplex DNA in solution, *Biochemistry 38*, 15425−15437.
40. Cao, Y., and He, X. (1998) Studies of interaction between Safranine T and double helix DNA by spectral methods, *Spectrochim. Acta*, *Part A 54*, 883−892.
41. Gábor, F., Szolnoki, J., Tóth, K., Fekete, A., Maillard, P., and Csík, G. (2001) Photo-induced inactivation of T7 phage sensitized by symmetrically and asymmetrically substituted tetraphenyl porphyrin: Comparison of efficiency and mechanism of action, *Photochem. Photobiol. 73*, 304−311.
42. Egyeki, M., Turóczy, G., Majer, Zs., Tóth, K., Fekete, A., Maillard, P., and Csík, G. (2003) Photosensitised Inactivation of T7 Phage as surrogate of non-enveloped DNA viruses. Efficiency and mechanism of action, *Biochim. Biophys. Acta 1624*, 115−124.

BI0495477